The Astrophysical Journal, 736:40 (13pp), 2011 July 20 doi:10.1088/0004-637X/736/1/40

COMPONENTS OF THE EXTRAGALACTIC GAMMA-RAY BACKGROUND

Floyd W. Stecker[1] and Tonia M. Venters[2,3]
[1] Astrophysics Science Division, NASA Goddard Space Flight Center, Greenbelt, MD 20771, USA; floyd.w.stecker@nasa.gov
[2] Goddard Space Flight Center, Greenbelt, MD 20771, USA
Received 2010 December 16; accepted 2011 April 23; published 2011 July 5

ABSTRACT

We present new theoretical estimates of the relative contributions of unresolved blazars and star-forming galaxies to the extragalactic γ-ray background (EGB) and discuss constraints on the contributions from alternative mechanisms such as dark matter annihilation and truly diffuse γ-ray production. We find that the *Fermi* source count data do not rule out a scenario in which the EGB is dominated by emission from unresolved blazars, though unresolved star-forming galaxies may also contribute significantly to the background, within order-of-magnitude uncertainties. In addition, we find that the spectrum of the unresolved star-forming galaxy contribution cannot explain the EGB spectrum found by EGRET at energies between 50 and 200 MeV, whereas the spectrum of unresolved flat spectrum radio quasars, when accounting for the energy-dependent effects of source confusion, could be consistent with the combined spectrum of the low-energy EGRET EGB measurements and the *Fermi*-Large Area Telescope EGB measurements.

Key words: galaxies: active – galaxies: general – gamma rays: diffuse background – gamma rays: galaxies

Online-only material: color figures

1. INTRODUCTION

Studies of the extragalactic γ-ray background (EGB) can provide insight into high-energy processes in the universe and, as such, has been the subject of much debate, particularly concerning the roles of extragalactic astrophysical sources and new physics. Recent data from the Large Area Telescope (LAT)[4] on board the *Fermi Gamma Ray Space Telescope* allow for a reassessment of the possible astrophysical origins of the EGB, which could improve our understanding of γ-ray production in these objects and provide more robust constraints on the more exotic scenarios. However, in order to determine the strength and spectrum of this isotropic background one needs to proceed from the raw photon count data by determining to the best extent possible the detector sensitivity, the intrinsic events produced by the larger charged particle flux impinging on the detector, and the much larger γ-ray foreground within our Galaxy resulting from cosmic-ray interactions with photons and gas nuclei. Such analyses have been made for both the Energetic γ-ray Experiment Telescope (EGRET) aboard the *Compton Gamma Ray Observatory* (Sreekumar et al. 1998; Strong et al. 2004a) and *Fermi* (Abdo et al. 2010j).

Various extragalactic γ-ray production scenarios have been explored theoretically as candidate components that could contribute significantly to the observed background. Among those considered are unresolved astronomical sources, such as active galactic nuclei (AGNs; Padovani et al. 1993; Stecker et al. 1993; Salamon & Stecker 1994; Chiang et al. 1995; Stecker & Salamon 1996; Kazanas & Perlman 1997; Chiang & Mukherjee 1998; Mukherjee & Chiang 1999; Mücke & Pohl 2000; Giommi et al. 2006; Narumoto & Totani 2006; Dermer 2007; Pavlidou & Venters 2008; Inoue & Totani 2009; Venters et al. 2009; Venters 2010; Abazajian et al. 2010), star-forming galaxies (Pavlidou & Fields 2002; Fields et al. 2010; Makiya et al. 2011), and starburst galaxies (Thompson et al. 2007; Stecker 2007; Makiya et al. 2011). The large majority of associated extragalactic sources detected thus far by both EGRET and *Fermi* are blazars (Hartmann et al. 1999; Abdo et al. 2010f), i.e., those AGNs for which the jet is closely aligned with the observer's line of sight (Blandford & Königl 1979), including γ-ray loud flat spectrum radio quasars (FSRQs) and BL Lacertae type objects. It is expected that since blazars comprise the largest class of identified extragalactic γ-ray sources, unresolved blazars should contribute significantly to the EGB. Additionally, just as our Galaxy produces γ-rays, it is expected that γ-rays are produced in other galaxies, and as such, unresolved galaxies might also contribute to the EGB with the most significant contribution originating from the population of actively star-forming galaxies (Stecker 1975; Pavlidou & Fields 2001, 2002; Fields et al. 2010; Makiya et al. 2011). Interesting truly diffuse mechanisms that could contribute to the EGB involve cosmic-ray interactions with intergalactic gas and the cosmic background radiation (Fazio et al. 1966; Stecker 1973; Dar 2007; Keshet et al. 2003) and electromagnetic cascades produced by interactions of very high and ultrahigh energy particles with the extragalactic background light (Kalashev et al. 2009; Berezinsky et al. 2011; Ahlers et al. 2010; Venters 2010), as well as more exotic scenarios such as dark matter annihilation (Silk & Srednicki 1984; Stecker et al. 1985; Rudaz & Stecker 1988; Stecker & Tylka 1989a, 1989b; Rudaz & Stecker 1991; Ullio et al. 2002) and decay (Olive & Silk 1985; Stecker 1986; Ibarra & Tran 2008).[5]

In this paper, we estimate the contributions to the EGB from unresolved extragalactic γ-ray sources of various types and compare them with the EGB obtained from analysis of *Fermi* data. In doing so, we also take into consideration the effects of both the completeness of the *Fermi* flux-limited blazar survey and the important effect of source confusion owing to the energy-dependent angular resolution of the *Fermi*-LAT detector. We will then briefly discuss the implications of possible truly diffuse emission mechanisms to the EGB.

[3] NASA Postdoctoral Program Fellow.
[4] Hereafter we shall refer to the *Fermi*-LAT instrument simply as *Fermi*.
[5] For reviews on dark matter annihilation, see Jungman et al. (1996) and Bertone et al. (2005).

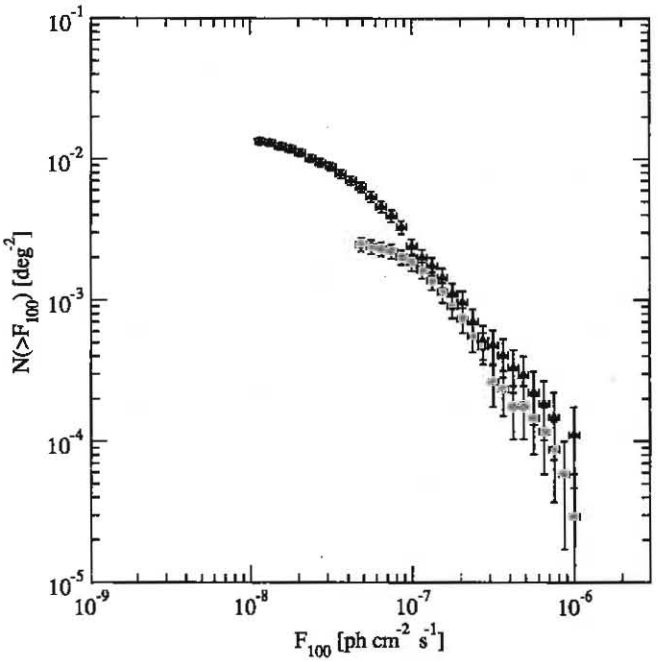

Figure 1. Source count distributions for *Fermi* (black triangles; Abdo et al. 2010f) and EGRET (red circles; Reimer & Thompson 2001) blazars.
(A color version of this figure is available in the online journal.)

2. EGRET AND *FERMI* RESOLVED SOURCES AND THE γ-RAY log N–log S RELATION

In Figure 1, we plot the number of blazars observed per square degree versus blazar flux integrated above 100 MeV for both EGRET (Reimer & Thompson 2001) and *Fermi* (Abdo et al. 2010f). In the case of *Fermi*, the source spectra were extrapolated from a power-law fit above a fiducial energy of 1 GeV (Abdo et al. 2010k). The offset between the resolved source count data obtained by the two detectors is a result of differences in their sensitivity calibrations (Thompson et al. 1993; Abdo et al. 2010f). The fluxes of the *Fermi* sources are reported to be systematically brighter than those reported by EGRET.

We note that the 50% completeness in the *Fermi* survey is estimated to be reached at an effective flux limit of $\sim 2 \times 10^{-8}$ cm^{-2} s^{-1} (Abdo et al. 2010k). The flux limit varies with galactic latitude and source hardness. Nevertheless, the effective flux limit indicated by both the turnover in Figure 1 and the Monte Carlo simulation in Abdo et al. (2010k) is $\sim 2 \times 10^{-8}$ cm^{-2} s^{-1}. By assuming that the *Fermi* survey is 100% complete at $\sim 7 \times 10^{-8}$ cm^{-2} s^{-1} (Abdo et al. 2010k) and comparing the data for EGRET and *Fermi* shown in Figure 1, we estimate that the EGRET survey is 50% complete at $\sim 8 \times 10^{-8}$ cm^{-2} s^{-1}.

One may note that the flux level attained for 50% completeness for the *Fermi* extragalactic blazar survey is only about four times fainter than that for the EGRET survey even though the *Fermi*-LAT is sensitive to sources ~30 times fainter than that of EGRET. It is important to note that there are several factors that determine the efficiency of a γ-ray telescope for detecting extragalactic sources, among which are (1) the flux of the source, (2) the spectral index of the source, (3) the intrinsic detector background from cosmic-ray-induced events, (4) the foreground from the Milky Way, and (5) the diffuse extragalactic background. The *Fermi*-LAT was designed to reach its optimal effective area for γ-rays with energies near and above 1 GeV, whereas EGRET was designed to reach its optimal effective area for γ-rays with energies near and above 100 MeV. As such, *Fermi* is more sensitive to sources with hard spectral indices, particularly for the faintest sources observable by *Fermi*. Thus, it is difficult to make a direct comparison between EGRET and *Fermi*. However, we note that the positions of the turnovers in the data presented in Figure 1 provide a good indication of the observational situation.

3. DETERMINATION OF THE EGB FROM POINT SOURCES

In general, the total contribution of a given population of sources to the EGB is found by convolving the source spectrum, $F_{\rm ph}(E_0, z, L_\gamma)$, measured at energy, E_0, of one source of γ-ray luminosity, L_γ, at a given redshift, z, with the comoving number density of sources at that redshift per luminosity interval, $n(L_\gamma, z) = d^2N/dL_\gamma dV_{\rm com}$. We then integrate over the comoving volume, $V_{\rm com}$, and γ-ray luminosity:

$$I_E(E_0) = \int_0^{z_{\rm max}} \int_{L_{\gamma,\rm min}}^{L_{\gamma,\rm max}} F_{\rm ph}(E_0, z, L_\gamma) n(L_\gamma, z) \frac{d^2V_{\rm com}}{dz d\Omega} dL_\gamma dz\,, \quad (1)$$

where $I_E(E_0)$ is the EGB intensity given in units of photons cm^{-2} s^{-1} sr^{-1} GeV^{-1}, $L_{\gamma,\rm max}$ depends on the redshift, source spectrum, and the detector sensitivity, and we have differentiated the comoving volume with respect to redshift and solid angle, Ω. However, as the different types of likely contributing γ-ray sources have distinct spectral characteristics and redshift and luminosity distributions, we must consider each case separately.

Note that in Equation (1) we have neglected the effect of γ-ray absorption due to pair-production interactions with the extragalactic UV photons. The inclusion of γ-ray absorption would result in a steepening in the collective point source spectrum at the high-energy end (Salamon & Stecker 1998; Venters et al. 2009), though a possible contribution from electromagnetic cascade photons might mitigate the steepening at higher energies (Venters 2010). However, recent *Fermi* constraints on the γ-ray opacity imply that the UV background is likely to be fairly low (Abdo et al. 2010e), and as such, the absorption and the resulting cascades will only have a small effect on the EGB.

3.1. The Contribution to the EGB from Unresolved Blazars

In determining the blazar contribution to the EGB, we follow the procedure outlined in Venters et al. (2009). We approximate the blazar γ-ray spectrum as a power law in energy defined by the *photon* spectral index, Γ ($F_{\rm ph} \propto E^{-\Gamma}$). The spectral indices of the population of blazars form a distribution with some spread (the spectral index distribution, SID; Stecker & Salamon 1996; Venters & Pavlidou 2007); hence, the number density of blazars is defined as

$$n(L_\gamma, z, \Gamma) = \rho_\gamma(L_\gamma, z) p_L(\Gamma) = \frac{d^3N}{dL_\gamma dV_{\rm com} d\Gamma}\,, \quad (2)$$

where $\rho_\gamma(L_\gamma, z) = d^2N/dL_\gamma dV_{\rm com}$ is the blazar γ-ray luminosity function (GLF) giving the comoving number density of blazars per luminosity interval and $p_L(\Gamma) = dN/d\Gamma$ is the normalized blazar SID accounting for spectral bias (see Section 4). L_γ is the γ-ray luminosity at the fiducial energy, E_f (taken to

be 100 MeV), defined as E_f^2 times the differential photon luminosity, $L_{\rm pl} = d^2N_\gamma/dtdE$ measured at E_f. L_γ is related to the integral flux greater than E_f, $F(>E_f)$, by

$$L_\gamma = 4\pi D^2(\Gamma - 1)(1+z)^\Gamma E_f F(>E_f), \quad (3)$$

where D is the distance measure for the Friedman–Robertson–Walker cosmology:[6]

$$D = \frac{c}{H_0}\int_0^z [\Omega_\Lambda + \Omega_m(1+z')^3]^{-1/2}\,dz'. \quad (4)$$

A given blazar of γ-ray luminosity, L_γ, at a redshift, z, with a γ-ray photon spectral index, Γ, has a measured photon flux of

$$F_{\rm ph}(E_0, z, L_\gamma, \Gamma) = \frac{L_\gamma}{4\pi E_f^2 [d_L(z)]^2}(1+z)^{2-\Gamma}\left(\frac{E_0}{E_f}\right)^{-\Gamma}, \quad (5)$$

where $d_L(z) = D(1+z)$ is the luminosity distance. Thus, the total contribution to the EGB at a given energy, E_0, from unresolved blazars (the collective unresolved blazar intensity) is determined by integrating the contribution from each individual blazar fainter than the detector sensitivity,

$$I_E^{\rm bl}(E_0) = \int_{-\infty}^{\infty}\int_0^{z_{\rm max}}\int_{L_{\gamma,\rm min}}^{L_{\gamma,\rm max}} F_{\rm ph}(E_0, z, L_\gamma, \Gamma)\rho_\gamma p_L(\Gamma) \times \frac{d^2V_{\rm com}}{dz d\Omega}\,dL_\gamma\,dz\,d\Gamma, \quad (6)$$

where $z_{\rm max} = 5.0$ and $L_{\gamma,\rm max}$ is determined from Equation (3) taking $F(>E_f) = F_{\rm min}$, with $F_{\rm min}$ being the minimum flux capable of being resolved by *Fermi*. We have also integrated Equation (1) over the blazar spectral index.

3.2. The Contribution to the EGB from Unresolved Star-forming Galaxies

By applying the same procedure that we use to determine the background from unresolved blazars (see Section 3.1), we calculate the contribution from unresolved star-forming galaxies by determining the γ-ray photon flux as a function of energy for one galaxy and then convolving with and integrating over the appropriate cosmological distributions. It is expected that, as in the Milky Way, the γ-ray emission for a star-forming galaxy comes mainly from the decay of π^0 mesons produced by cosmic-ray interactions with interstellar gas (Stecker 1970). The resulting γ-ray production spectrum has been calculated by many authors (Stecker 1970, 1973, 1979; Cavallo & Gould 1971; Stephens & Badhwar 1981; Dermer 1986; Mori 1997; Strong et al. 2004b, 2007, 2010; Kelner et al. 2006; Kamae et al. 2006; Mori 2009). For our calculation, we adopt the π^0 emissivity given by Stecker (1979) renormalized upward by 25% to be consistent with the local emissivity measured by *Fermi* (Abdo et al. 2009b). We note that there is also emission arising from electron bremsstrahlung, but the contribution is likely to be small, particularly above 100 MeV (Abdo et al. 2009b). We also neglect the emission from Compton interactions that may contribute significantly to galaxy spectra above 10 GeV, particularly for starburst galaxies (Stecker 1977; Hunter et al. 1997; Abdo et al. 2009b; Strong et al. 2010). We also note that the cosmic-ray spectrum should, in fact, vary from galaxy to galaxy since it depends on energy-dependent leakage and each galaxy has a different morphology and magnetic field configuration. This uncertainty can affect the predicted slope of the EGB spectrum at high energies, but it does not affect the absolute value of the predicted background at ~200 MeV.

The γ-ray photon luminosity is related to the γ-ray production spectrum per hydrogen atom, $q_{\rm H}(E)$, by

$$L_{\rm ph}(E) = \langle q_{\rm H}(E)\rangle\, N_{\rm H}, \quad (7)$$

where $\langle q_{\rm H}(E)\rangle$ is found by averaging $q_{\rm H}(E)$, the differential γ-ray production spectrum per hydrogen atom, over the galaxy, and $N_{\rm H}$ is the number of hydrogen atoms in the galaxy in the form of both atomic (H I) and molecular (H_2) hydrogen. Thus, the γ-ray photon flux for a galaxy at redshift z as observed at energy E_0 is

$$F_{\rm ph}(E_0, z) = \frac{1}{4\pi D^2}\langle q_{\rm H}[E_0(1+z)]\rangle\, N_{\rm H}(z). \quad (8)$$

The rate of production of γ-rays from π^0 decay is proportional to the flux of cosmic rays, which we assume to be proportional to the supernova rate. The supernova rate is expected to be proportional to the rate of formation of higher mass stars, which is, in turn, proportional to the overall star formation rate (SFR) assuming a universal initial mass function (IMF).

Assuming then that the rate of production of γ-rays from π^0 decay is proportional to the SFR for a galaxy, we can relate the $\langle q_{\rm H}\rangle$ of the galaxy to that of the Milky Way, $\langle q_{\rm H}^{\rm MW}\rangle$:

$$\frac{\langle q_{\rm H}\rangle}{\langle q_{\rm H}^{\rm MW}\rangle} = \frac{\Psi(z)}{\Psi(z=0)}, \quad (9)$$

where Ψ is the SFR of the galaxy, and we take $\langle q_{\rm H}^{\rm MW}\rangle$ to be some fraction, f_q, of the locally measured[7] $q_{\rm H}^{\rm MW}$. We determine f_q by integrating the radial profile of the flux of cosmic rays weighted by r^2. Using the radial profiles calculated by Stecker & Jones (1977), we obtain $f_q \sim 0.825$. Thus, the galaxy spectrum becomes

$$F_{\rm ph}(E_0, z) = \frac{1}{4\pi D^2} f_q q_{\rm H}^{\rm MW}[E_0(1+z)]\frac{\Psi(z)}{\Psi(0)}N_{\rm H}(z). \quad (10)$$

The calculation of the amount of gas in a galaxy is subject to a considerable degree of uncertainty, especially at high redshifts (see Section 4.2). As such, rather than focusing on one particular model, we calculate the star-forming galaxy contribution for three different models arising from different sets of assumptions. In so doing, we seek to explore various possibilities and highlight the uncertainty.

3.2.1. Galaxy Contribution Determined from the Schechter Function and An Evolving Gas Fraction

One method for determining the number of hydrogen atoms in a galaxy is to assume that the mass of gas in the galaxy is some fraction of its stellar mass:

$$N_{\rm H}(z) = \frac{f_{\rm gas}(z)}{1 - f_{\rm gas}(z)}\frac{M_*}{m_{\rm H}}, \quad (11)$$

where $f_{\rm gas}(z) = M_{\rm gas}/(M_{\rm gas} + M_*) \propto (1+z)^{0.9}$ is the gas fraction given in Papovich et al. (2011), and we have neglected

[6] We take $H_0 = 70$ km s^{-1} Mpc^{-1}, $\Omega_m = 0.3$, $\Omega_\Lambda = 0.7$, and $\Omega_r \ll 1$.

[7] That is, since $q_{\rm H}^{\rm MW}$ is calculated in the literature assuming the cosmic-ray flux as measured in the solar neighborhood.

the possible contribution of helium to the gas mass of a galaxy. Substituting Equation (11) into Equation (10) and approximating $\Psi(z)/\Psi(0) \sim \dot{\rho}_{\rm SFR}(z)/\dot{\rho}_{\rm SFR}(0)$, we get

$$F_{\rm ph}(E_0, z, M_*) = \frac{f_q q_{\rm H}^{\rm MW}[E_0(1+z)]}{4\pi m_{\rm H} D^2} \frac{\dot{\rho}_{\rm SFR}(z)}{\dot{\rho}_{\rm SFR}(0)} \frac{f_{\rm gas}(z)}{1-f_{\rm gas}(z)} M_*, \quad (12)$$

where $\dot{\rho}_{\rm SFR}(z)$ is the cosmic SFR (CSFR) given by $\log(\dot{\rho}_{\rm SFR}(z)) = -2.06 + 3.39\log(1+z)$ for $z < 1.3$ and $\dot{\rho}_{\rm SFR}(z) \sim$ const. for $1.3 \leqslant z \leqslant 4.0$ (Ly et al. 2011).

To get the total contribution to the EGB, we convolve with the comoving number density of star-forming galaxies per stellar mass interval as a function of redshift and integrate

$$I_E^{\rm gal}(E_0) = \int_0^{z_{\rm max}} dz \frac{d^2 V_{\rm com}}{dz d\Omega} \times \int_{M'_{\rm min}}^{M'_{\rm max}} dM' F_{\rm ph}(E_0, z, M')\Phi(z, M'), \quad (13)$$

where $\Phi(z, M') = d^2N/dM'dV_{\rm com}$ is the Schechter function for stellar mass with parameters as determined in Elsner et al. (2008), M' is given by $M_* = 10^{M'} M_\odot$, and we take $M'_{\rm min} = 8.0$ and $M'_{\rm max} = 12.0$.

3.2.2. Galaxy Contribution Determined from IR Luminosity Functions

Alternatively, we can determine the γ-ray spectrum of a galaxy by assuming that the γ-ray luminosity of the galaxy is proportional to some power of its SFR (Fields et al. 2010; Makiya et al. 2011; Abdo et al. 2010g): $L_{\rm ph} \propto \Psi^\alpha$. Since $L_{\rm ph}(E) = \langle q_{\rm H}(E)\rangle N_{\rm H}$ and $\langle q_{\rm H}(E)\rangle \propto \Psi$ (as demonstrated in Section 3.2.1),

$$N_{\rm H} = \left(\frac{A\Psi_{\rm MW}}{\int |q_{\rm H}^{\rm MW}(E)| dE}\right)\Psi^{\alpha-1}, \quad (14)$$

where A and α are the best-fit parameters of the above power law determined from *Fermi* observations of star-forming galaxies in the Local Group and their SFRs (see Section 4.2.2). Assuming the Chabrier (2003) IMF, the SFR of a galaxy is related to its total infrared luminosity, $L_{\rm IR}$,

$$L_{\rm IR} = 1.1 \times 10^{10} L_\odot \left(\frac{\Psi}{M_\odot\ {\rm yr}^{-1}}\right) \quad (15)$$

(Hopkins et al. 2010). The γ-ray photon flux for a galaxy at redshift z is given by

$$F_{\rm ph}(E_0, z, L_{\rm IR}) = \frac{1}{4\pi D^2}\left(\frac{A}{\int q_{\rm H}^{\rm MW} dE}\right) \times \left(\frac{L_{\rm IR}}{1.1\times 10^{10} L_\odot}\right)^\alpha q_{\rm H}^{\rm MW}[E_0(1+z)]. \quad (16)$$

Then, the total contribution to the EGB is found by convolving the galaxy photon flux with an infrared luminosity function, $\Phi(z, L_{\rm IR}) = d^2N/dL_{\rm IR}dV_{\rm com}$ and integrating over infrared luminosity and redshift:

$$I_E^{\rm gal}(E_0) = \int_0^{z_{\rm max}} dz \frac{d^2 V_{\rm com}}{dz d\Omega} \times \int_{L_{\rm IR,min}}^{L_{\rm IR,max}} dL_{\rm IR} F_{\rm ph}(E_0, z, L_{\rm IR})\Phi(z, L_{\rm IR}), \quad (17)$$

where we take $L_{\rm IR,min} = 10^{10} L_\odot$ and $L_{\rm IR,max} = 10^{15} L_\odot$.

3.2.3. Galaxy Contribution Determined from the Cosmic Star Formation Rate and the Star Formation Efficiency

Another alternative is to relate the cosmic density of hydrogen in star-forming galaxies to the cosmic SFR. Given that stars are formed in giant molecular clouds (GMCs), it is reasonable to assume

$$\dot{\rho}_{\rm SFR} \sim \xi({\rm H}_2)\rho_{\rm H_2}, \quad (18)$$

where $\dot{\rho}_{\rm SFR}$ is the cosmic SFR density (see Section 3.2.1), $\rho_{\rm H_2}$ is the cosmic molecular hydrogen density in star-forming galaxies, and $\xi({\rm H}_2)$ is the star formation "efficiency" (SFE) of molecular hydrogen (Bigiel et al. 2008; Gnedin et al. 2009; Bauermeister et al. 2010). Leroy et al. (2008) measure the SFE to be $\sim(5.25 \pm 2.5) \times 10^{-10}\ {\rm yr}^{-1}$ and to be roughly constant over a wide range of conditions.[8] We can relate the density of atomic hydrogen to the density of molecular hydrogen through the average mass ratio of atomic and molecular hydrogen ($\mathcal{R} = \langle M_{\rm H\,I}/M_{\rm H_2}\rangle$) in star-forming galaxies, $\rho_{\rm H\,I} \sim \mathcal{R}\rho_{\rm H_2}$. The average mass ratio of atomic and molecular hydrogen can be found by integrating radial profiles of the gas surface densities of star-forming galaxies found in Leroy et al. (2008), resulting in $\mathcal{R} \sim 0.9$. Note that in doing so, we only integrate the profiles out to the optical radius since recent surveys indicate that star formation is extremely inefficient beyond this radius (Bigiel et al. 2010).[9] Thus, with appropriate modifications to Equation (10), we find the γ-ray flux from a particular redshift

$$F_{\rm ph}(E_0, z) = \frac{f_q(1+\mathcal{R})}{4\pi m_{\rm H}\xi({\rm H}_2)D^2} q_{\rm H}^{\rm MW}[E_0(1+z)] \frac{\dot{\rho}_{\rm SFR}^2(z)}{\dot{\rho}_{\rm SFR}(0)} \frac{dV_{\rm com}}{dz} dz. \quad (19)$$

Differentiating with respect to solid angle Ω and integrating over redshift results in an equation for the total contribution to the EGB:

$$I_E^{\rm gal}(E_0) = \frac{f_q(1+\mathcal{R})}{4\pi m_{\rm H}\xi({\rm H}_2)\dot{\rho}_{\rm SFR}(0)} \int_0^{z_{\rm max}} \times \frac{1}{D^2} q_{\rm H}^{\rm MW}[E_0(1+z)]\dot{\rho}_{\rm SFR}^2(z)\frac{d^2V_{\rm com}}{d\Omega dz} dz. \quad (20)$$

4. OBSERVATIONAL INPUTS AND CONSIDERATIONS

4.1. γ-ray Blazars

Of the nearly 1500 resolved point sources observed by *Fermi* in the first year, 573 are associated with blazars (First *Fermi* catalog (1FGL); Abdo et al. 2010f). Thus, blazars comprise the largest class of astrophysical objects associated with γ-ray sources. Naturally, unresolved blazars have long been suspected of providing, at least, a substantial contribution to the EGB, though the exact amount remains debatable and depends on various assumptions as to constructing GLFs and redshift distributions (Padovani et al. 1993; Stecker et al. 1993; Salamon & Stecker 1994; Chiang et al. 1995; Stecker & Salamon 1996;

[8] More precisely, $\xi({\rm H}_2) \sim \epsilon/\tau_{\rm ff}$, where ϵ is the percentage of gas involved in forming stars and $\tau_{\rm ff} \propto \rho^{-1/2}$ is the *local* free-fall timescale of the gas. However, using this relation requires knowledge of the local density of the gas and a better understanding of the formation of GMCs than presently exists (see Section 4.2). We also note that the measurements obtained by Leroy et al. (2008) were taken from a sample of low-redshift galaxies. The SFE could actually evolve with redshift (Bauermeister et al. 2010).

[9] We should note that even though star formation is extremely inefficient beyond the isophotal radius, there is still gas beyond this radius. However, based on the radial profiles determined in Stecker & Jones (1977), we do not expect cosmic rays to propagate much beyond the isophotal radius; hence, we expect gamma-ray production beyond this radius to be low.

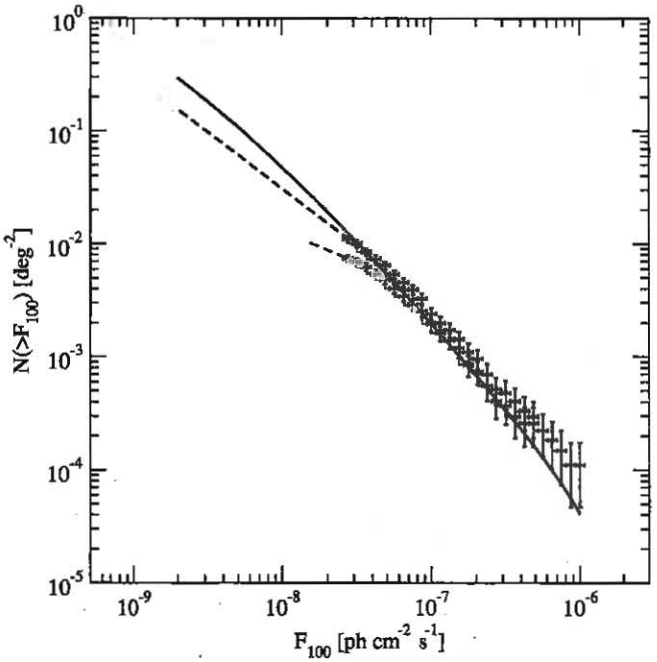

Figure 2. Bright end of the source count distributions for all blazars (including BL Lac objects; black data points) and FSRQs (light green data points). Our model fit to the data is shown by the solid (purple) line. The dashed lines are the faint-end slopes determined in Abdo et al. (2010k) by including a modeled Monte Carlo *Fermi*-LAT efficiency.

(A color version of this figure is available in the online journal.)

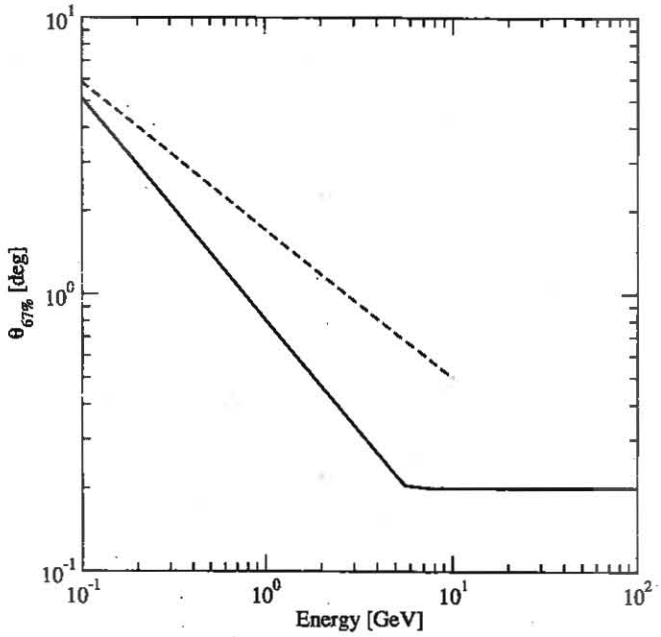

Figure 3. Angular resolution as a function of energy for the *Fermi*-LAT (solid black line; Atwood et al. 2009) and EGRET (dashed red line; Thompson et al. 1993).

(A color version of this figure is available in the online journal.)

Kazanas & Perlman 1997; Chiang & Mukherjee 1998; Sreekumar et al. 1998; Mukherjee & Chiang 1999; Mücke & Pohl 2000; Giommi et al. 2006; Narumoto & Totani 2006; Dermer 2007; Kneiske & Mannheim 2008; Pavlidou & Venters 2008; Inoue & Totani 2009; Venters et al. 2009; Abdo et al. 2010k; Venters 2010). A detailed discussion of all of the assumptions that go into these calculations is beyond the scope of this paper (though, for a detailed discussion of the Chiang & Mukherjee 1998 calculation, see Stecker & Salamon 2001), and it is likely that many of these models will be updated in light of *Fermi* data. However, we note that as discussed in Abdo et al. (2010k), the source counts predicted by Dermer (2007) and Mücke & Pohl (2000) fall short of the *Fermi* observations of resolved sources above 5×10^{-8} photons cm^{-2} s^{-1}. In calculating the blazar contribution to the EGB, we assume functional forms for the blazar GLF and SID and fit them to 1FGL data, accounting for errors in measurement of blazar spectral indices and the spectral bias inherent in a flux-limited catalog.

4.1.1. Source Counts for Faint Unresolved Blazars: Theory Meets Observations

Determining the GLF from observations relies on the ability to associate γ-ray blazars with lower energy counterparts for which redshifts can be measured (for a discussion, see Venters et al. 2009; Venters 2010). However, making the necessary association can be complicated by the angular resolution of the *Fermi*-LAT, which is limited by electron scattering in the LAT detector and is much poorer than that of more traditional telescopes (see Figure 3). The resulting wide point-spread function results in significant source confusion at energies below ~1 GeV even for fluxes well above the *Fermi*-LAT sensitivity. In principle, one could construct source counts from fluxes integrated above an energy for which source confusion is less of a hindrance, but doing so would limit the already suppressed blazar number statistics. Thus, rather than construct a luminosity function solely from γ-ray blazars with redshifts, we employ the Stecker & Salamon (1996)[10] approach of determining the luminosity function from wavebands with larger samples and smaller positional error circles.

As in Stecker & Salamon (1996), we take the functional form of the FSRQ luminosity function from radio observations (Dunlop & Peacock 1990), but corrected for the present cosmological parameters. The γ-ray luminosity of a blazar is then determined from its radio luminosity. The average correlation between the radio and γ-ray luminosities of blazars is determined by fitting the bright end of modeled source counts[11] to that of the observed γ-ray source counts ($\chi^2_{\rm reduced} \sim 0.4$). In so doing, we find that the γ-ray luminosity integrated from 100 MeV to 100 GeV is $\sim 10^{3.2}$ times νL_ν in radio, in agreement with the results obtained using recent *Fermi* observations[12] (Giroletti et al. 2010; Abdo et al. 2010j; Ghirlanda et al. 2011; Mahony et al. 2010). We should also note that we include sources out to $z \sim 5$, but as demonstrated in Venters et al. (2009), the emission is dominated by sources with $z \lesssim 2$ (consistent with expectations from the redshift distribution predicted by the GLF). As

[10] See also Narumoto & Totani (2006).

[11] In doing so, we also include the blazar SID (see Section 4.1.3).

[12] One might be concerned that the effect of the new radio–γ correlation would be to increase the blazar background with respect to the Stecker & Salamon (1996) model. However, we note that Stecker & Salamon (1996) distinguished between "quiescent" and "flaring" blazars and used separate radio–γ correlations (and spectral properties) for each subpopulation. In this paper, we make no such distinction, so a comparison between our results and those of the Stecker & Salamon (1996) model is not straightforward. Using the Stecker & Salamon (1996) radio–γ correlation for quiescent blazars from Stecker & Salamon (1996) would yield a smaller blazar background, but it would also underpredict the bright end of the γ-ray source counts. To compensate, one would have to add a flaring component (as per Stecker & Salamon 1996) to fit the data, which would also contribute to the background. In effect, such a procedure is equivalent to our method of fitting the radio–γ correlation to the data.

such, we do not expect this choice to significantly impact the results.

The resulting modeled source count distribution for FSRQs (solid) is presented in Figure 2 along with the distributions of the brighter FSRQs resolved by *Fermi* (light data points) and all blazars (dark data points). We also show the forms of the unresolved source count distributions obtained from a Monte Carlo modeled *Fermi*-LAT sensitivity calculation performed by Abdo et al. (2010k) as dashed lines. All of the models separate from the data at fainter fluxes as the source counts fall off very rapidly due to the survey incompleteness and source confusion. Thus, the determination of the *true* faint-end shape directly from the source counts can be severely hindered.

In an effort to mitigate the effect of survey completeness, Abdo et al. (2010k) modeled the *Fermi*-LAT efficiency from a Monte Carlo simulation and then divided the differential source counts by this efficiency. Thus, the calculated source counts for faint sources strongly depend on such modeled efficiencies. Indeed, at fluxes near the *Fermi*-LAT sensitivity limit, the efficiency is extremely small and model dependent; hence, in flux bins with low number statistics, the source counts are multiplied by a very large and uncertain number. The result of such a procedure is that even though one source is not statistically different from two sources, whether one source is seen or two could result in different modeled counts for faint sources. It has also been argued that unassociated γ-ray sources are likely to be dominated by known classes of γ-ray sources, especially blazars (Mirabal et al. 2010) and will have a contribution to the EGB even though they will not have been included in the source count distributions. It is also important to note that in determining the blazar contribution to the EGB from measured source count distributions, source confusion could not be taken into account since its effect depends on the source density (see Section 4.1.2), which is exactly the unknown quantity that the observer seeks to determine. As such, it is likely that the blazar contribution to the EGB will be underestimated in analyses based solely on the measured source count distributions. Since in this paper we use a theoretically determined source count distribution, our model gives a source count density from which one can determine the effect of source confusion (see Section 4.1.2). Such differences between our analysis and that given in Abdo et al. (2010k) result in different calculations of the unresolved blazar contribution to the EGB: Abdo et al. (2010k) conclude that blazars can only account for less than 25% of the EGB,[13] while our analysis indicates that blazars could possibly account for the bulk of the EGB.

The F_{100} fluxes included in the source count distributions presented in Figure 1 are not actually *measured* F_{100} fluxes since the 1FGL catalog does not include F_{100} fluxes. In order to determine the F_{100} fluxes, we make use of Equation (1) of Abdo et al. (2010k) to *extrapolate* F_{100} fluxes from measured differential fluxes determined at the pivot energies. Abdo et al. (2010f) define the pivot energy as that energy for which the differential flux is minimal. We note that for 1FGL blazars, the average of the pivot energies is $\sim$1 GeV. Thus, the source count distributions might be more representative of source counts for sources brighter than the *Fermi* sensitivity above 1 GeV rather than 100 MeV. In effect (and also as the result of spectral bias; see Section 4.1.3), the source counts could underestimate the number of blazars with F_{100} fluxes above the *Fermi* sensitivity, mostly impacting the faint end of the source count distributions. As such, analyses on unresolved blazars based solely on source counts likely underestimate the blazar contribution to the EGB. This effect could provide an explanation for the fact that *Fermi* observes roughly as many BL Lac objects as FSRQs even though BL Lac objects are intrinsically fainter than FSRQs. Since the γ-ray spectra of BL Lac objects are harder than those of FSRQs they are more easily observed by *Fermi* than FSRQs.

4.1.2. The Fermi-LAT and EGRET Angular Resolutions and Source Confusion

As mentioned previously, the large angular resolutions of pair-production γ-ray detectors such as EGRET and the *Fermi*-LAT[14] result in significant source confusion, particularly for faint sources and for energies below $\sim$1 GeV. Since the angular resolution for the *Fermi*-LAT is similar to that of EGRET at $\sim$100–200 MeV, the capability of *Fermi* to resolve faint sources is similar to that of EGRET at these energies. Hence, if the EGB does indeed consist of unresolved sources, then the EGB measurements of the detectors should be similar at $\sim$100–200 MeV, whereas at $\sim$1 GeV, the improved angular resolution of *Fermi* with respect to that of EGRET should result in a lower measurement of the EGB by *Fermi* than that of EGRET owing to the enhanced ability of *Fermi* to resolve point sources (Stecker & Salamon 1999).

The probability, $\mathcal{P}$, of finding a nearest neighboring source with $S \geqslant S_{\rm lim}$ within the minimum angular separation, $\theta_{\rm min}$, for a source density, N, is given by

$$\mathcal{P}(\leqslant \theta_{\rm min}(E)) = 1 - \exp\left(-\pi N \theta^2_{\rm min}(E)\right). \quad (21)$$

For our source confusion criterion, we take the acceptable probability limit, $\mathcal{P}_{\rm min} \sim 0.1$, and $\theta_{\rm min}(E) \sim \theta_{67\%}(E)$ approximately given by

$$\theta_{67\%}(E) = 5.^{\circ}12 \times \left(\frac{E}{100\,{\rm MeV}}\right)^{-0.8} \quad (22)$$

(Atwood et al. 2009; see Figure 3). Then, the source density criterion (SDC) is found by inverting Equation (21):

$$N_{\rm SDC} = -\frac{\ln(1-\mathcal{P}_{\rm min})}{\pi \theta^2_{\rm min}(E)}. \quad (23)$$

The limiting source flux, $S_{\rm SDC}$, is then determined from the modeled source counts.

If one were to think of the *Fermi*-LAT as an ordinary telescope with $\theta_{\rm min} = \theta_{67\%}$ where $\theta_{67\%}$ is the half-angle for a beam that contains 67% of the photons, the SDC would correspond to $\sim$1/10 sources per beam. For sources with $F_{100} \lesssim 1 \times 10^{-7}$ photons cm^{-2} s^{-1}, the probability for finding another γ-ray source of similar or greater flux within the error circle is quite high; hence, many sources that, in principle, should be resolvable are, in fact, *unresolved*. At fluxes close to the sensitivity limit, this probability is so high that faint sources are *indistinguishable* and will contribute to the measured EGB of the detector in question (for the *Fermi*-LAT resolution at 100 MeV, the source criterion corresponds to $N_{\rm SDC} \sim 1.3 \times 10^{-3}$ sources deg^{-2}; for reference, at $F \sim 2 \times 10^{-9}$ photons cm^{-2} s^{-1}, our model predicts a much larger source density of $\sim$0.3 sources deg^{-2}). Thus, the effect of source

[13] In Section 8 of Abdo et al. (2010k) a value of 40% of the EGB is obtained if one extrapolates to zero flux.

[14] See http://www-glast.slac.stanford.edu/software/IS/glast_lat_performance.htm.

confusion compounded with the separate effect of detector sensitivity is to flatten the faint end of an observationally derived source count distribution.

We should emphasize that this definition of source confusion is not the same as that employed by Abdo et al. (2010k). Source confusion as discussed in this section refers to the probability that for a given source density, a source has a nearest neighbor within the angular resolution of the detector with a flux greater than or equal to the flux limit. In Abdo et al. (2010k), the term is applied to a *detected* source associated with a given *real* source for which the measured flux of the detected source is greater than the flux of the real source (plus three standard deviations) by a given amount (the analysis was performed on simulated data to determine the impact on the actual data). In effect, the former definition identifies the limit at which the source density is sufficiently large so that individual sources *cannot* be resolved, and only fluctuations are observed. The latter definition applies to the probability that a given detected source is in fact the superposition of several sources. However, the Abdo et al. (2010k) criterion is based on the assumption that a source can be *resolved*. As such, the source would have to be significantly brighter than the background, including the sources within the error circle of the detector. In the case when many sources have similar fluxes, none of the sources would be resolved. In the case of one bright source and several fainter sources, the flux of the detected source would be dominated by the flux of the brightest source, leading to an overestimate of the flux of the dominant source and an undercount of the fainter source in the Abdo et al. (2010k) analysis. Thus, under this criterion, it is not surprising that they conclude that there is very little source confusion. A common treatment of source confusion in measured source counts is a fluctuation analysis, but as yet, such an analysis has not been performed on *Fermi* source counts.

4.1.3. Blazar Spectra

The spectral indices of the population of blazars form a distribution with a given finite spread (Stecker & Salamon 1996; Venters & Pavlidou 2007), resulting in a curvature in the spectrum of the collective intensity of unresolved blazars due to the increasing relative importance at high energies of blazars with harder spectral indices (Stecker & Salamon 1996; Pavlidou & Venters 2008). Thus, the determination of the blazar SID is crucial in determining the correct spectrum of the unresolved blazar contribution.

In determining the blazar SID from survey data, one must carefully account for uncertainties in measurement of the spectral indices. In so doing, we follow the likelihood method of Venters & Pavlidou (2007), fitting *Fermi* 1FGL FSRQs to a Gaussian SID. We determined the maximum-likelihood Gaussian SID parameters (mean, Γ_0, and spread, σ_0) to be $\Gamma_0 = 2.45$ and $\sigma_0 = 0.15$.

We must also account for the effect of spectral bias of the 1FGL catalog. Even in a flux-limited catalog, low-luminosity, high-redshift blazars that would be most likely to appear are those with spectral indices that are harder than most of the population. The 1FGL catalog is not actually flux limited (see Section 2); rather, it consists of sources above a given threshold in test statistic,[15] which depends on source spectra and the background. However, as demonstrated in Venters & Pavlidou (2010), applying the likelihood analysis to the sample of FSRQs with fluxes $\gtrsim 7 \times 10^{-8}$ photons cm^{-2} s^{-1} and galactic latitudes $\gtrsim 10°$ (as per Abdo et al. 2010k) does not appreciably change the SID parameters ($\Gamma_0 = 2.45$, $\sigma_0 = 0.16$).[16] Thus, even though the 1FGL catalog is not flux limited, we can assume that the sample of 1FGL FSRQs is approximately flux limited. We can then follow the method of Venters et al. (2009) in correcting for the sample bias inherent in a flux-limited catalog. In doing so, we apply a correction factor, $\hat{M}(\alpha)$, to the SID (for derivation, see Venters et al. 2009):

$$p_L(\alpha) = \frac{\hat{p}(\alpha)}{\hat{M}(\alpha)}, \tag{24}$$

where $\hat{p}(\alpha)$ is the SID corrected for measurement uncertainty in the spectral indices, and

$$\hat{M}(\alpha) \propto \int_{F_{\gamma,\min}}^{\infty} dF_\gamma \frac{1}{F_\gamma} \int_{z=0}^{\infty} dz \hat{p}_\gamma(\alpha, z, F_\gamma) \frac{dV_{\rm com}}{dz}(z). \tag{25}$$

4.1.4. Summary of Differences with the Stecker & Salamon (1996) Blazar Model

To summarize, our approach in calculating the blazar contribution to the EGB is similar to that of Stecker & Salamon (1996) with some notable differences.

1. The model has been updated to make use of the current cosmological parameters. The change in cosmology has little impact on the results.
2. The model considers only FSRQs, and flaring blazars are not considered separately from quiescent blazars. (For possible impact, see item 3.)
3. The γ-ray–radio relation has been updated to be consistent with multi-wavelength observations of FSRQs conducted by *Fermi* and radio telescopes ($L_\gamma \sim 10^{3.2} \times \nu L_\nu$ as opposed to $10^{2.6}$; see Section 4.1.1). As noted in Section 4.1.1, the smaller γ-ray–radio relation would result in a model that cannot by itself fit the data and would require a flaring component. In effect, this is, on average, equivalent to our choice of a single population of blazars with a given γ-ray–radio relation. We do not expect this choice to have a major impact on our results. However, as we will discuss in Section 4.1.5, the blazar duty cycle is a remaining uncertainty, and it could impact predictions for the number of blazars that are observable by *Fermi*.
4. The model has been updated to account for the effect of source confusion in the blazar contribution to the EGB (see Sections 4.1.2 and 5). As will be shown in Section 5, this has the effect of increasing the blazar background at lower energies.
5. The SID of FSRQs has been updated following the analysis of Venters & Pavlidou (2007; $\Gamma_0 = 2.45$, $\sigma_0 = 0.15$) and correcting for spectral bias as in Venters et al. (2009; see Section 4.1.3). Thus, the collective spectrum of blazars is not as hard as that presented in Stecker & Salamon (1996) and does not exhibit as much curvature.

4.1.5. Remaining Questions

There remain a few open questions, the answers to which will impact the determination of the blazar contribution to the EGB. The blazar duty cycle, which dictates the amount of time a blazar

[15] For 1FGL, this threshold is 25, corresponding to a statistical significance of $\sim 4\sigma$.

[16] See also Abdo et al. (2010k).

spends in the quiescent state versus the flaring state, remains uncertain, as do questions of the amount the flux increases during flaring and whether the spectral index changes during flaring. Analyses of EGRET blazar spectral indices found no evidence of systematic changes in spectral index with flaring (Nandikotkur et al. 2007; Venters & Pavlidou 2007), and *Fermi* observations of individual blazars have thus far revealed no systematic changes in spectral index with time or flux (Abdo et al. 2009c, 2010d; Ackermann et al. 2010b). As such, we are justified in assuming that the blazar spectral index remains constant, on average, with time. However, we acknowledge that the uncertainty of blazar variability parameters could have an impact on the counts of faint blazars and the γ-ray–radio correlation. This uncertainty will decrease as more data from *Fermi* become available.

Another open question is that of the nature of blazar spectra over the entire *Fermi* energy range. We treat blazar spectra as unbroken power laws over this range and in many observed blazars, this does appear to be a reasonable approximation. However, in at least a few cases, *Fermi* has found evidence that blazar spectra can break (Abdo et al. 2009a, 2010i, 2010l). Whether such observations are representative of the entire blazar population is presently unclear, as is the nature of the breaks. In any case, spectral breaks are likely to impact the collective unresolved blazar spectrum mostly at the high end of the *Fermi* energy range. It is also possible that the spectra of harder blazars[17] will compensate for that of softer blazars at higher energies (Venters & Pavlidou 2010).

4.2. Star-forming Galaxies

As discussed in Section 3.2, the Milky Way is a source of substantial γ-ray emission arising primarily from the decay of π^0 meson produced in inelastic collisions of cosmic rays with interstellar gas. Thus, it is expected that other star-forming galaxies emit γ-rays through the same interactions and that unresolved star-forming galaxies could provide a substantial contribution to the EGB. Thus far, the *Fermi*-LAT Collaboration has reported detections of two nearby irregular galaxies (the Small Magellanic Cloud (SMC) and the Large Magellanic Cloud (LMC); Abdo et al. 2010c, 2010h), two starburst galaxies (M82 and NGC253; Abdo et al. 2010b), and M31, a galaxy similar to our own (Abdo et al. 2010g). As such, whatever the contribution to the EGB from unresolved star-forming galaxies, it will not have changed substantially in the *Fermi* data with respect to EGRET data as *Fermi* has resolved only a handful of star-forming galaxies.

The determination of the star-forming galaxy contribution relies on knowledge of the SFR of galaxies and their gas content, both of which are subject to substantial observational and theoretical uncertainties. At relatively low redshifts ($z \lesssim 1.5$), nebular and forbidden emission lines (e.g., Hα, O II, and O III) can be used to trace star formation in galaxies.[18] At higher redshifts ($z \sim 1$–5), the redshifted UV continuum is used. However, both observational techniques are subject to uncertainties in dust extinction and the stellar IMF. Alternatively, in noting that UV radiation from young stars is absorbed by interstellar dust and reradiated in the infrared, measurements of the far-infrared (FIR) continuum can be used to trace star formation. Nevertheless, early-type galaxies can exhibit substantial FIR emission possibly due to dust heating by older stars or AGNs. Furthermore, infrared measurements are hindered by emission from our own Galaxy. Given these factors, the large degree of scatter present in the measurements (about a factor of a few; Le Borgne et al. 2009; Ly et al. 2011) of the CSFR density is not surprising.

The gas content of galaxies is even more uncertain, particularly at high redshift. The amount of H_2 in a galaxy is determined from measurements of CO emission, while H I is determined from measurements of the 21 cm line. However, the CO-to-H_2 conversion varies depending on the metallicity and radiation field of a given region and the opacity of the molecular clouds containing CO. The 21 cm surveys, on the other hand, extend only out to $z \sim 0.05$. At higher redshifts, measurements of the H I density of the universe rely on damped Lyα absorbers observed in the Lyα forest of quasar spectra, but the nature of these systems is still the subject of much debate (see, e.g., Kulkarni et al. 2010; Péroux et al. 2011). Furthermore, the connection between the total gas and SFR is complex (Putman et al. 2009). While it is fairly well established that stars form in GMCs and hence that star formation traces H_2, the amount of H I varies between galaxies and does not appear to be correlated with star formation (Bigiel et al. 2008; Leroy et al. 2008). From both the observational and the theoretical points of view, the transition from H I to H_2 and the formation of GMCs remain uncertain (Leroy et al. 2008).

Given the uncertainty surrounding key elements of the determination of the star-forming galaxy contribution to the EGB, our approach does not focus on a particular model. Instead, we employ several families of models that rely on separate sets of assumptions each with advantages and caveats. Using this approach, we seek to explore various possibilities for the star-forming galaxy contribution and highlight the uncertainty in such a calculation. The strategies we employ are summarized as follows.

1. Relate the galaxy gas mass to its stellar mass assuming a gas fraction that evolves with redshift.
2. Relate the galaxy γ-ray luminosity to its SFR, which, in turn, is related to an observable for which there is a redshift distribution (e.g., IR luminosity).
3. Relate the cosmic density of gas in star-forming galaxies to the SFR density.

4.2.1. The Schechter Function Model

In this approach, we relate the galaxy gas mass to its stellar mass assuming an evolving gas fraction (for details of the model, see Section 3.2.1). We employ the Schechter parameters of the stellar mass functions as determined by Elsner et al. (2008) and the evolving gas fraction as determined by Papovich et al. (2011). Since extensive spectroscopic surveys are, as yet, unavailable, Elsner et al. (2008) make use of combined data from the multi-band photometry of the GOODS-MUSIC catalog and the *Spitzer Space Telescope*. In so doing, they infer the stellar masses of galaxies from photometric data by fitting the mass-to-light ratios of galaxies to stellar population templates. Such a procedure is subject to a considerable degree of uncertainty, particularly arising from that of dust extinction[19] and the usage of photometric redshifts. Elsner et al. (2008) estimate the mean uncertainty in their stellar mass estimates to be about a factor

[17] We do not include a possible contribution from BL Lac objects for lack of a comparable radio data set.

[18] For a review of observational techniques of measuring star formation, see Kennicutt (1998).

[19] In order to mitigate the effect of the uncertainty in dust extinction, Elsner et al. (2008) make use of K_S-band M/L ratios since dust absorption is small for longer wavelengths.

Table 1
Observables for Local Group Galaxies

ID[a]	L_γ (photons s^{-1})	Ψ ($M_\odot$ yr^{-1})
SMC	$(1.7 \pm 0.3) \times 10^{40}$	$0.01 \pm (4.8 \times 10^{-4})$
LMC	$(7.8 \pm 0.6) \times 10^{40}$	$0.1 \pm (4.6 \times 10^{-3})$
M31	$(6.6 \pm 1.4) \times 10^{41}$	0.4 ± 0.18
Milky Way	$(1.2 \pm 0.2) \times 10^{42}$	0.93 ± 0.34
NGC 253	$(1.1 \pm 0.7) \times 10^{43}$	2.7 ± 0.5
M82	$(2.5 \pm 0.9) \times 10^{43}$	$5.4 \pm (5.9 \times 10^{-4})$

Note. [a] SMC: L_γ from Abdo et al. (2010c). SFR from Lawton et al. (2010) corrected for IMF. LMC: L_γ from Abdo et al. (2010h). SFR from Lawton et al. (2010) corrected for IMF. M31: L_γ from Abdo et al. (2010g). SFR from Tabatabaei & Berkhuijsen (2010) and Williams (2003) corrected for IMF. MW: L_γ calculated for $\langle q_H \rangle \sim 1.4 \times 10^{-25}$ s^{-1} H^{-1} and $M_H \sim 7 \times 10^9$ $M_\odot$ (Boissier & Prantzos 1999). SFR taken from Robitaille & Whitney (2010) corrected for IMF. NGC 253: L_γ from Abdo et al. (2010b). SFR from IR measurements given by Sanders et al. (2003). M82: L_γ from Abdo et al. (2010b). SFR from IR measurements given by Sanders et al. (2003). Note that the errors in the SFRs reflect only statistical uncertainties and assume that Equation (15) is exactly correct.

of two, though they did not estimate the possible uncertainty resulting from the usage of photometric redshifts.

Papovich et al. (2011) study the relationship between the SFR and stellar mass of high-redshift galaxies selected at a constant comoving number density and derive a gas fraction that evolves[20] as $(1 + z)^{0.9}$. They estimate that the uncertainty on the gas mass is ~0.11 dex.

The advantage of this kind of model is that it is based on observations that will be continuously refined with time. However, we note that the relationship between the stellar mass of a galaxy and its total gas content is unclear, though perhaps with better observations and a better theoretical understanding, the relationship will be better determined.

4.2.2. The IR Luminosity Function Models

In this approach, we assume that the γ-ray luminosity of a star-forming galaxy can be related to its SFR as a power law. In order to determine this relationship, we fit γ-ray luminosities of Local Group galaxies calculated from *Fermi* measurements[21] to their SFRs either taken from the literature or calculated from IR measurements and converted to SFR via Equation (15). In all cases, the SFR is calculated assuming (or corrected to) the IMF of Chabrier (2003). We find the best-fit power law to be given by L_γ (10^{41} photons s^{-1}) $\sim 24.0 \times \Psi^{1.2}$. This fit is consistent with that obtained by the *Fermi* Collaboration, $L_\gamma \propto \Psi^{1.4 \pm 0.3}$ (Abdo et al. 2010g). Observables for Local Group galaxies used in this analysis are given in Table 1 and plotted with the fit in Figure 4. In a manner similar to that of blazars, we can relate the γ-ray luminosity of a star-forming galaxy to its total IR luminosity, convolve with an IR luminosity function, and integrate with respect to IR luminosity and redshift.

While the use of IR luminosity functions taken from observations is possible, it is difficult to deconvolve the contributions from obscured AGNs and mergers. As such, we use the semi-empirical IR luminosity functions determined from the halo-occupation-based methodology of Hopkins et al. (2010)

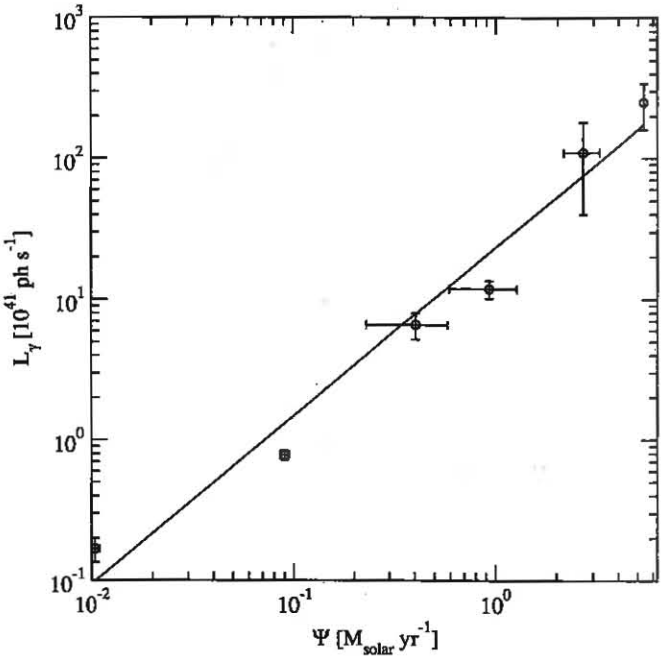

Figure 4. γ-ray luminosities of Local Group galaxies plotted vs. their star formation rates (data points; see Table 1). Also plotted is the power-law fit relating the γ-ray luminosity to the SFR (solid red line): $L_\gamma \propto \Psi^{1.2}$.
(A color version of this figure is available in the online journal.)

for both star-forming and starburst galaxies (in which enhanced star formation due to major mergers is taken into account).[22] While the Hopkins et al. (2010) IR luminosity functions match available observations fairly well, we note that there is considerable debate over the roles of AGNs and mergers in driving star formation, the evolution of galaxies, and the determination of the IR luminosities of massive systems. Furthermore, the γ-ray–SFR correlation is based on rather uncertain estimates of the SFRs and γ-ray luminosities of one normal galaxy (our own), two irregular galaxies, and two starburst galaxies, all of which could, in principle, exhibit different star formation properties. As more data become available from *Fermi*, the γ-ray–SFR correlation will be further tested. If it proves robust, then studies of the normal galaxy contribution to the EGB could have implications for large-scale-structure formation and the evolution of galaxies with cosmic time.

4.2.3. The Strong Coupling γ-ray–Star Formation Rate Model

In this approach, we seek to relate the cosmic density of hydrogen in star-forming galaxies to the cosmic SFR. Observations of nearby galaxies have indicated that localized star formation traces the density of H_2 but there is no direct correlation with H I (Bigiel et al. 2008; Leroy et al. 2008). While, in principle, there should be some relationship between the amount of H I, the amount of H_2, and the SFR in a galaxy, other factors such as density fluctuations and turbulence make such a relationship complex. Therefore, while acknowledging that the relationship between H I and SFR is unclear, we simply assume that the amount of H I in star-forming galaxies is, *on average*, comparable to that of H_2 within the optical radius

[20] Note that we extrapolate the functional form of their gas fraction to low redshifts.

[21] For the Milky Way, we calculate the γ-ray luminosity from q_H averaged over the whole galaxy (as discussed in Section 3.2) and the M_H taken from Boissier & Prantzos (1999).

[22] Note that we do not consider any contribution from the so-called calorimetry effect for starburst galaxies as such an effect is likely to be small (Stecker 2007). We have assumed the same form of the π^0-decay spectrum for starburst galaxies as for star-forming galaxies.

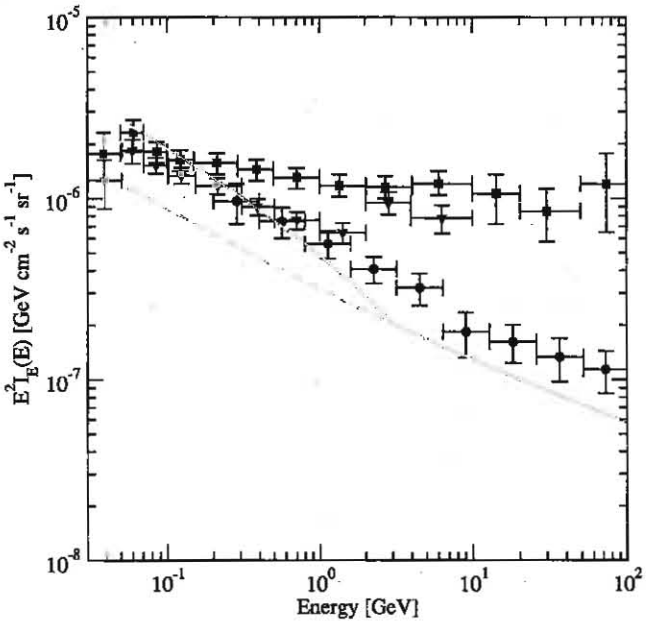

Figure 5. Collective spectrum of unresolved FSRQs. Solid green line: the spectrum accounting for source confusion. Dashed green line: the spectrum without accounting for source confusion. Black circles: the *Fermi* measurement of the spectrum of the EGB as determined in Abdo et al. (2010j). Blue squares: the EGRET measurement of the spectrum of the EGB as determined by Sreekumar et al. (1998) and confirmed by the analysis of Stecker et al. (2008) and S. D. Hunter (2011, private communication). Red triangles: the EGRET measurement of the spectrum of the EGB as determined by Strong et al. (2004a).

(A color version of this figure is available in the online journal.)

of the galaxy (see Section 3.2.3). Hence, in this model, we take the γ-ray luminosity to be roughly proportional to the *square* of the SFR. We stress that the assumption that the SFR is proportional to the available gas density only applies to galaxies that are actively forming stars. This assumption does not apply to galaxies at very high redshifts which may contain substantial amounts of gas but have yet to begin forming stars. However, we only include star-forming galaxies out to $z \sim 4$, so the higher redshift galaxies will not impact on our results. Given that the best-fit power-law index determined for Local Group galaxies in Section 4.2.2 is $\sim$1.2 and given the proximity of the resulting unresolved spectrum to the *Fermi* measurements of the EGB (see Section 5), we consider this model to be reflective of an upper limit to the star-forming galaxy contribution to the EGB.

4.3. The Fermi Spectrum and Unresolved Sources Versus Truly Diffuse Mechanisms

The *Fermi* observations have placed significant constraints on extragalactic dark matter annihilation (Cirelli et al. 2010; Abdo et al. 2010a; Ackermann et al. 2010a). Currently, there is no evidence of quark-annihilation features and spectral lines seen in the EGB spectrum, features that would be a clear annihilation signal (see, e.g., Stecker & Tylka 1989a; Rudaz & Stecker 1991). The observed spectrum does not match that expected from dark matter annihilation, placing constraints on any dark matter annihilation contribution to the EGB (Abdo et al. 2010a). Therefore, it is probable that dark matter annihilation γ-rays, if present, provide only a minor contribution to the EGB.

The same argument about matching spectra can be made regarding the contribution from electromagnetic cascades produced by very high and ultrahigh energy cosmic-ray interactions as the resulting spectrum would be significantly harder than the observed spectrum (Kalashev et al. 2009; Berezinsky et al. 2011; Ahlers et al. 2010; Venters 2010).

5. RESULTS

The calculated spectrum of the unresolved FSRQ contribution to the EGB (see Sections 3.1 and 4.1) is plotted in Figure 5. For comparison, we include the *Fermi* analysis of the EGB (Abdo et al. 2010j), two analyses[23] of the EGRET EGB (Sreekumar et al. 1998; Strong et al. 2004a), and the calculation of the collective spectrum of unresolved FSRQs ignoring the effect of source confusion. Our results clearly show that the effect of source confusion is to reduce the number of resolved sources, increasing the collective intensity of unresolved blazars, particularly below $\sim$1 GeV energy. Thus, accounting for source confusion modifies the predicted spectrum such that the EGRET and *Fermi* measurements of the EGB below $\sim$1 GeV are both compatible with unresolved FSRQs. In contrast, the better angular resolution of the *Fermi*-LAT above $\sim$ 1 GeV allows it to resolve more blazars resulting in a limiting flux that is dominated by the *Fermi*-LAT sensitivity rather than source confusion. Thus, the collective spectrum of FSRQs breaks at $\sim$3 GeV.[24] At energies above $\sim$1 GeV, the predicted collective spectrum of FSRQs falls below the data points, though they are likely consistent with the data within the uncertainties in the galactic foreground emission model. Note also that the collective FSRQ spectrum exhibits much less curvature than seen in Stecker & Salamon (1996). This is because the spread in the SID in our current model is much smaller than that of the Stecker & Salamon (1996) model.

In Figure 6, we plot the spectra of the unresolved star-forming galaxy contributions to the EGB calculated for the models discussed in Sections 3.2 and 4.2. For comparison, we include the spectrum of the unresolved starburst galaxy contribution alone that we determined from the best-fit IR luminosity function of Hopkins et al. (2010). For the spectrum of starburst galaxies, we have assumed the same form of the π^0-decay spectrum as for star-forming galaxies. The range in the calculations of the overall contribution to the EGB from unresolved star-forming galaxies spans about an order of magnitude, indicating the degree of uncertainty in such a calculation.[25]

We note that even though our most extreme model could possibly explain the lowest energy *Fermi* data points (and possibly, within systematics, a couple other), it cannot explain the EGRET data points below 300 MeV. The Strong et al. (2004a) EGRET data points (minus the two highest energy data points) with the *Fermi* data points resemble a *featureless* power law, while the spectra of unresolved star-forming galaxies do not. Notably, the data points show no indication of a π^0-decay

[23] The two sets of EGRET data points result from two different estimations of the galactic foreground emission.

[24] The actual break should be more gradual since in our calculations we used the approximate broken angular resolution curve shown in Figure 3.

[25] However, we note that each individual model is subject to its own uncertainty. As such, the degree of uncertainty is likely even more than an order of magnitude. Within the range of our various predictions of the EGB from star-forming galaxies, we agree with the results of the model of Fields et al. (2010) and Makiya et al. (2011).

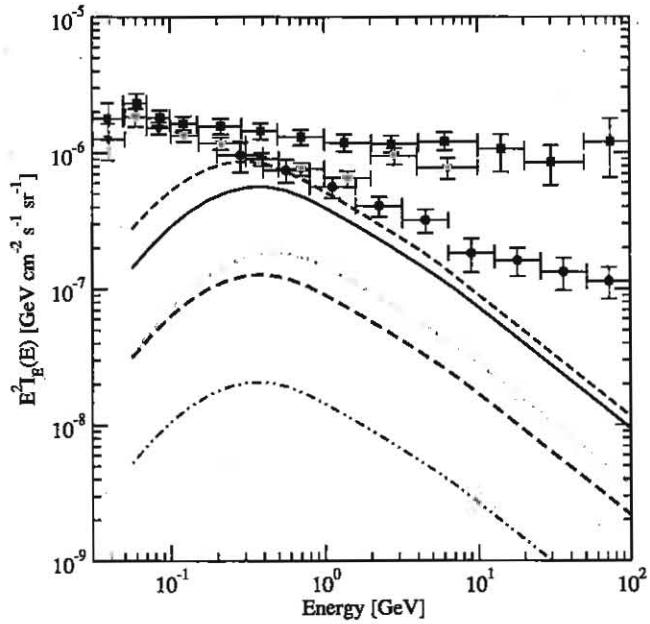

Figure 6. Collective spectrum of unresolved star-forming galaxies. Dashed indigo line: the spectrum determined from the strong coupling model (see Sections 3.2.3 and 4.2.3). Solid blue line: the spectrum determined from the IR luminosity function model (see Sections 3.2.2 and 4.2.2). Dot-dashed yellow line: the spectrum determined from the IR luminosity function model assuming no gas evolution. Dashed red line: the spectrum determined from the Schechter function model (see Sections 3.2.1 and 4.2.1). Double dot-dashed line: the spectrum of the starburst contribution alone determined from the IR luminosity function model.

(A color version of this figure is available in the online journal.)

"bump" at the energies at which the contribution of the star-forming galaxies should peak.

6. DISCUSSION AND CONCLUSIONS

We have calculated the spectral shape of the contribution of unresolved FSRQs to the EGB assuming that the γ-ray luminosity of an FSRQ is, on average, proportional to its radio luminosity (Giroletti et al. 2010; Abdo et al. 2010j; Ghirlanda et al. 2011; Mahony et al. 2010), and also accounting for the effects of source confusion. We have demonstrated that the combination of the source density predicted by the Dunlop & Peacock (1990) FSRQ radio luminosity function and the strong energy dependence of the *Fermi*-LAT angular resolution *increases* the contribution of unresolved FSRQs to the EGB at energies below 1 GeV. The resulting overall spectrum predicted by the fit to the *Fermi* source count distribution reproduces well the spectrum of the EGRET and *Fermi* EGB measurements below 1 GeV, but falls below the data points above 1 GeV. We have also calculated the spectral shape of the contribution of unresolved star-forming galaxies to the EGB for several relations for the γ-ray luminosity of a star-forming galaxy. We find that, depending on the model, the overall amount of the contribution of star-forming galaxies to the EGB may be more or less significant, though regardless of the model considered, the spectrum of unresolved star-forming galaxies is unable to explain the combined spectrum of the low-energy EGRET EGB measurements and the *Fermi* EGB measurements. Similar calculations for starburst galaxies alone indicate that they account for at most about 1% of the EGB, in agreement with the conclusion reached by Stecker (2007).

The similarity of the collective spectrum of unresolved FSRQs to the combined spectrum of the EGRET and *Fermi* EGB measurements, as demonstrated by our results, is striking. In fact, we note that as predicted in Stecker & Salamon (1999), the inclusion of the effect of source confusion in the calculation could provide an explanation for the similarity between the EGRET and *Fermi* EGB measurements at energies of hundreds of MeV. The density of FSRQs predicted by the model is sufficiently large such that at these energies, *Fermi* would not be able to resolve many more FSRQs than EGRET did, and the FSRQ contribution to the EGB would remain the same for *Fermi* as for EGRET. Thus, if unresolved FSRQs *do* comprise the bulk of the EGB emission, then one would expect such a similarity between the EGRET and *Fermi* measurements at these energies. At energies above 1 GeV, the *Fermi*-LAT angular resolution improves substantially with respect to that of EGRET, and as such, *Fermi* would be able to resolve more blazars at higher energies than EGRET could, resulting in a decrease in the *Fermi* EGB with respect to the EGRET EGB, an effect which is possibly indicated by comparing the EGRET and *Fermi* results.[26]

In contrast, no such high-energy separation between the EGRET EGB and the *Fermi* EGB is predicted for star-forming galaxies as all but the closest are too faint to be resolvable by *Fermi*. Furthermore, we note that the EGRET EGB measurements provide no indication of a turnover in the spectrum as would be expected if unresolved star-forming galaxies comprise the bulk of the EGB emission. Rather, the spectrum of unresolved star-forming galaxies is *inconsistent* with the combined spectrum of the EGRET and *Fermi* EGB measurements.[27] We also note that the lack of a turnover in the EGRET data is not simply the result of systematics (S. D. Hunter 2011, private communication), since the uncertainties in all of the galactic foreground models used to determine the EGB from the EGRET and *Fermi* data are quite small at these energies. Finally, we note that at energies above ~1 GeV, the spectrum of unresolved star-forming galaxies is steeper than the spectra of the EGB data. As such, we conclude that however significant the contribution of star-forming galaxies to the EGB may be, it is not sufficient to explain the EGB.[28]

Within the range of our various predictions of the EGB from star-forming galaxies, we agree with the results of the models of both Fields et al. (2010; which suggests that star-forming galaxies may comprise the bulk of the EGB) and Makiya et al. (2011; which suggests that star-forming galaxies can account

[26] A caveat is that the uncertainties in the subtraction of the galactic foreground emission at the higher energies are considerable owing to the uncertainty in the distributions of both gas and cosmic rays in the Galaxy. Furthermore, the instrumental backgrounds of EGRET and the *Fermi*-LAT are different, so it is difficult to make a direct comparison between the two. We should also note that in our calculations, we have neglected the population of BL Lac objects, which, due to their hard spectra, are likely to have more of a contribution at energies above ~10 GeV. Notably, *Fermi* has resolved as many BL Lac objects as FSRQs.

[27] As previously noted, the *Fermi*-LAT was designed to reach its optimal effective area for γ-rays with energies near and above ~1 GeV, whereas EGRET was designed to reach its optimal effective area for γ-rays with energies near and above ~100 MeV. Also, the *Fermi*-LAT detector has a significantly higher instrumental background at 100 MeV than EGRET did (S. D. Hunter 2011, private communication). Thus, the EGB was not reported by *Fermi* for energies below 200 MeV (Abdo et al. 2010j).

[28] The effect of Compton interactions mentioned in Section 3.2 does not alter this conclusion as it only modifies the spectrum above 10 GeV for normal galaxies (Strong et al. 2010) and the starburst galaxy contribution to the EGB is negligible. (See Figure 6.)

for less than 10% of the EGB). This underscores the range of uncertainty in the calculation for star-forming galaxies.[29]

The featureless spectrum of the EGB deduced by *Fermi* is intriguing when one considers the possibility of features that could arise from phenomena such as breaks in blazar spectra, absorption of high-energy γ-rays from unresolved blazars, γ-ray emission from unresolved star-forming galaxies, γ-ray emission from dark matter annihilation, and γ-rays from electromagnetic cascades initiated by very high and ultrahigh energy particle interactions with the extragalactic background light. The spectra of these potential contributions to the EGB differ considerably from that of the FSRQs (Silk & Srednicki 1984; Stecker et al. 1985; Rudaz & Stecker 1988; Stecker & Tylka 1989a, 1989b; Rudaz & Stecker 1991; Ullio et al. 2002; Ando et al. 2007; Kalashev et al. 2009; Siegal-Gaskins & Pavlidou 2009; Berezinsky et al. 2011; Ahlers et al. 2010; Venters 2010). However, recent *Fermi* observations have placed significant constraints on dark matter annihilation (Cirelli et al. 2010; Abdo et al. 2010a; Ackermann et al. 2010a), and presently there is no clear evidence of annihilation features above the background continuum. As such, it appears that any putative contribution to the EGB from dark matter annihilation is relatively minor. The possible contribution to the EGB from electromagnetic cascades is constrained by the relative steepness of the EGB spectrum, though cascades could play a role at higher energies (Kalashev et al. 2009; Berezinsky et al. 2011; Ahlers et al. 2010; Venters 2010). An apparent explanation for the featureless power-law spectrum of the EGB as presently deduced could be that unresolved blazars provide the dominant contribution to the EGB, given that their collective spectrum is roughly consistent with that of the EGB.

Therefore, we conclude that, contrary to the result given by Abdo et al. (2010k), the *Fermi* observations do not rule out the possibility that the EGB is dominated by emission from unresolved blazars.

We thank David Thompson, Stan Hunter, and Olaf Reimer for discussions of the EGRET detector characteristics and EGRET data. We thank Marco Ajello for sending the results of his Monte Carlo simulations of the *Fermi*-LAT efficiency versus source flux. We also thank Dawn Erb for comments regarding the infrared surveys of star-forming galaxies at high redshifts and Matt Malkan, Vasiliki Pavlidou, Jane Rigby, and the anonymous referee for helpful discussions. T.M.V. acknowledges support by an appointment to the NASA Postdoctoral Program at the Goddard Space Flight Center, administered by Oak Ridge Associated Universities through a contract with NASA.

REFERENCES

Abazajian, K. N., Blanchet, S., & Harding, J. P. 2010, arXiv:1012.1247
Abdo, A. A., et al. 2009a, ApJ, 700, 597
Abdo, A. A., et al. 2009b, ApJ, 703, 1249
Abdo, A. A., et al. 2009c, ApJ, 697, 934
Abdo, A. A., et al. 2010a, J. Cosmol. Astropart. Phys., JCAP04(2010)014
Abdo, A. A., et al. 2010b, ApJ, 709, L152
Abdo, A. A., et al. 2010c, A&A, 523, A46
Abdo, A. A., et al. 2010d, ApJ, 721, 1425
Abdo, A. A., et al. 2010e, ApJ, 723, 1082
Abdo, A. A., et al. 2010f, ApJS, 188, 405
Abdo, A. A., et al. 2010g, A&A, 523, L2
Abdo, A. A., et al. 2010h, A&A, 512, A7
Abdo, A. A., et al. 2010i, ApJ, 710, 1271
Abdo, A. A., et al. 2010j, Phys. Rev. Lett., 104, 101101
Abdo, A. A., et al. 2010k, ApJ, 720, 435
Abdo, A. A., et al. 2010l, ApJ, 716, 30
Ackermann, M., et al. 2010a, J. Cosmol. Astropart. Phys., JCAP05(2010)025
Ackermann, M., et al. 2010b, ApJ, 721, 1383
Ahlers, M., et al. 2010, Astropart. Phys., 34, 106
Ando, S., Komatsu, E., Narumoto, T., & Totani, T. 2007, Phys. Rev. D, 75, 063519
Atwood, W. B., et al. 2009, ApJ, 697, 1071
Bauermeister, A., Blitz, L., & Ma, C. 2010, ApJ, 717, 323
Berezinsky, V., Gazizov, A., Kachelrieß, M., & Ostapchenko, S. 2011, Phys. Lett. B, 695, 13
Bertone, G., Hooper, D., & Silk, J. 2005, Phys. Rep., 405, 279
Bigiel, F., Leroy, A., Walter, F., Blitz, L., Brinks, E., de Blok, W. J. G., & Madore, B. 2010, AJ, 140, 1194
Bigiel, F., Leroy, A., Walter, F., Brinks, E., de Blok, W. J. G., Madore, B., & Thornley, M. D. 2008, AJ, 136, 2846
Blandford, R. D., & Königl, A. 1979, ApJ, 232, 34
Boissier, S., & Prantzos, N. 1999, MNRAS, 307, 857
Cavallo, G., & Gould, R. J. 1971, Nuovo Cimento B, 2B, 77
Chabrier, G. 2003, PASP, 115, 763
Chiang, J., Fichtel, C. E., von Montigny, C., Nolan, P. L., & Petrosian, V. 1995, ApJ, 452, 156
Chiang, J., & Mukherjee, R. 1998, ApJ, 496, 752
Cirelli, M., Panci, P., & Serpico, P. D. 2010, Nucl. Phys. B, 840, 284
Dar, A. 2007, Nucl. Phys. B (Proc. Suppl.), 165, 103
Dermer, C. D. 1986, A&A, 157, 223
Dermer, C. D. 2007, ApJ, 659, 958
Dunlop, J. S., & Peacock, J. A. 1990, MNRAS, 247, 19
Elsner, F., Feulner, G., & Hopp, U. 2008, A&A, 477, 503
Fazio, G. G., Stecker, F. W., & Wright, J. P. 1966, ApJ, 144, 611
Fields, B. D., Pavlidou, V., & Prodanović, T. 2010, ApJ, 722, L199
Ghirlanda, G., Ghisellini, G., Tavecchio, F., Foschini, L., & Bonnoli, G. 2011, MNRAS, 413, 853
Giommi, P., Colafrancesco, S., Cavazzuti, E., Perri, M., & Pittori, C. 2006, A&A, 445, 843
Giroletti, M., Reimer, A., Fuhrmann, L., Pavlidou, V., & Richards, J. L. 2010, in ASP Conf. Ser. 427, Accretion and Ejection in AGN: A Global View, ed. L. Maraschi et al. (San Francisco, CA: ASP), 283
Gnedin, N. Y., Tassis, K., & Kravtsov, A. V. 2009, ApJ, 697, 55
Hartmann, R. C., et al. 1999, ApJS, 123, 79
Hopkins, P. F., Younger, J. D., Hayward, C. C., Narayanan, D., & Hernquist, L. 2010, MNRAS, 402, 1693
Hunter, S. D., et al. 1997, ApJ, 481, 205
Ibarra, A., & Tran, D. 2008, Phys. Rev. Lett., 100, 061301
Inoue, Y., & Totani, T. 2009, ApJ, 702, 523
Jungman, G., Kamionkowski, M., & Griest, K. 1996, Phys. Rep., 267, 195
Kalashev, O. E., Semikoz, D. V., & Sigl, G. 2009, Phys. Rev. D, 79, 063005
Kamae, T., Karlsson, N., Mizuno, T., Abe, T., & Koi, T. 2006, ApJ, 647, 692
Kazanas, D., & Perlman, E. 1997, ApJ, 476, 7
Kelner, S. R., Aharonian, F. A., & Bugayov, V. V. 2006, Phys. Rev. D, 74, 034018
Kennicutt, R. C., Jr. 1998, ARA&A, 36, 189
Keshet, U., Waxman, E., Loeb, A., Springel, V., & Hernquist, L. 2003, ApJ, 585, 128
Kneiske, T. M., & Mannheim, K. 2008, A&A, 479, 41
Kulkarni, V. P., Khare, P., Som, D., Meiring, J., York, D. G., Péroux, C., & Lauroesch, J. T. 2010, New Astron., 15, 735
Lawton, B., et al. 2010, ApJ, 716, 453
Le Borgne, D., Elbaz, D., Ocvirk, P., & Pichon, C. 2009, A&A, 504, 727
Leroy, A. K., Walter, F., Brinks, E., Bigiel, F., de Blok, W. J. G., Madore, B., & Thornley, M. D. 2008, AJ, 136, 2782
Ly, C., Lee, J. C., Dale, D. A., Momcheva, I., Salim, S., Staudaher, S., Moore, C. A., & Finn, R. 2011, ApJ, 726, 109
Mahony, E. K., Sadler, E. M., Murphy, T., Ekers, R. D., Edwards, P. G., & Massardi, M. 2010, ApJ, 718, 587
Makiya, R., Totani, T., & Kobayashi, M. A. R. 2011, ApJ, 728, 158

[29] One noteworthy difference between our model and that of Fields et al. (2010) is that in order to relate the gas mass of a galaxy to its star formation rate, Fields et al. (2010) make use of the Schmidt–Kennicutt relation. However, in doing so, they estimate the disk sizes of galaxies to high redshifts. Given that the uncertainties in these quantities are likely to be considerable (and given the uncertainty already present in the calculation), we considered alternative approaches. Nevertheless, we note that the Schmidt–Kennicutt relation was included in the inputs to both the IR luminosity models and the Schechter function model. In the IR luminosity model, we tested the impact of changing the Schmidt–Kennicutt law by performing the calculation for the Hopkins et al. (2010) IR luminosity function calculated using a steeper Schmidt–Kennicutt relation and found that it had very little impact on our results.

Mirabal, N., Nieto, D., & Pardo, S. 2010, arXiv:1007.2644
Mori, M. 1997, ApJ, 478, 225
Mori, M. 2009, Astropart. Phys., 31, 341
Mücke, A., & Pohl, M. 2000, MNRAS, 312, 177
Mukherjee, R., & Chiang, J. 1999, Astropart. Phys., 11, 213
Nandikotkur, G., Jahoda, K. M., Hartman, R. C., Mukherjee, R., Sreekumar, P., Böttcher, M., Sambruna, R. M., & Swank, J. H. 2007, ApJ, 657, 706
Narumoto, T., & Totani, T. 2006, ApJ, 643, 81
Olive, K. A., & Silk, J. 1985, Phys. Rev. Lett., 55, 2362
Padovani, P., Ghisellini, G., Fabian, A. C., & Celotti, A. 1993, MNRAS, 260, L21
Papovich, C., Finkelstein, S. L., Ferguson, H. C., Lotz, J. M., & Giavalisco, M. 2011, MNRAS, 412, 1123
Pavlidou, V., & Fields, B. D. 2001, ApJ, 558, 63
Pavlidou, V., & Fields, B. D. 2002, ApJ, 575, L5
Pavlidou, V., & Venters, T. M. 2008, ApJ, 673, 114
Péroux, C., Bouché, N., Kulkarni, V. P., York, D. G., & Vladilo, G. 2011, MNRAS, 410, 2237
Putman, M. E., et al. 2009, arXiv:0902.4717
Reimer, O., & Thompson, D. J. 2001, Proc. 27th ICRC (Hamburg), 2566
Robitaille, T. P., & Whitney, B. A. 2010, ApJ, 710, L11
Rudaz, S., & Stecker, F. W. 1988, ApJ, 325, 16
Rudaz, S., & Stecker, F. W. 1991, ApJ, 368, 406
Salamon, M. H., & Stecker, F. W. 1994, ApJ, 430, L21
Salamon, M. H., & Stecker, F. W. 1998, ApJ, 493, 547
Sanders, D. B., Mazzarella, J. M., Kim, D., Surace, J. A., & Soifer, B. T. 2003, AJ, 126, 1607
Siegal-Gaskins, J. M., & Pavlidou, V. 2009, Phys. Rev. Lett., 102, 241301
Silk, J., & Srednicki, M. 1984, Phys. Rev. Lett., 53, 624
Sreekumar, P., et al. 1998, ApJ, 494, 523
Stecker, F. W. 1970, Ap&SS, 6, 377
Stecker, F. W. 1973, Nature Phys. Sci., 241, 74
Stecker, F. W. 1975, Phys. Rev. Lett., 35, 188
Stecker, F. W. 1977, ApJ, 212, 60
Stecker, F. W. 1979, ApJ, 228, 919
Stecker, F. W. 1986, Phys. Rev. Lett., 56, 2551
Stecker, F. W. 2007, J. Phys.: Conf. Ser., 60, 215
Stecker, F. W., Hunter, S. D., & Kniffen, D. A. 2008, Astropart. Phys., 29, 25
Stecker, F. W., & Jones, F. C. 1977, ApJ, 217, 843
Stecker, F. W., Rudaz, S., & Walsh, T. F. 1985, Phys. Rev. Lett., 55, 2622
Stecker, F. W., & Salamon, M. H. 1996, ApJ, 464, 600
Stecker, F. W., & Salamon, M. H. 1999, Proc. 26th ICRC (Salt Lake City), 313
Stecker, F. W., & Salamon, M. H. 2001, in AIP Conf. Proc. 587, Gamma 2001: Gamma-Ray Astrophysics, ed. S. Ritz, N. Gehrels, & C. R. Shrader (Melville, NY: AIP), 432
Stecker, F. W., Salamon, M. H., & Malkan, M. A. 1993, ApJ, 410, L71
Stecker, F. W., & Tylka, A. J. 1989a, ApJ, 336, L51
Stecker, F. W., & Tylka, A. J. 1989b, ApJ, 343, 169
Stephens, S. A., & Badhwar, G. D. 1981, Ap&SS, 76, 213
Strong, A. W., Moskalenko, I. V., & Ptuskin, V. S. 2007, Annu. Rev. Nucl. Part. Sci., 57, 285
Strong, A. W., Moskalenko, I. V., & Reimer, O. 2004a, ApJ, 613, 956
Strong, A. W., Moskalenko, I. V., & Reimer, O. 2004b, ApJ, 613, 962
Strong, A. W., et al. 2010, ApJ, 722, L58
Tabatabaei, F. S., & Berkhuijsen, E. M. 2010, A&A, 517, A77
Thompson, T. A., Quataert, E., & Waxman, E. 2007, ApJ, 654, 219
Thompson, D. J., et al. 1993, ApJS, 86, 629
Ullio, P., Bergström, L., Edsjö, J., & Lacey, C. 2002, Phys. Rev. D, 66, 123502
Venters, T. M. 2010, ApJ, 710, 1530
Venters, T. M., & Pavlidou, V. 2007, ApJ, 666, 128
Venters, T. M., & Pavlidou, V. 2010, arXiv:1105.0372
Venters, T. M., Pavlidou, V., & Reyes, L. C. 2009, ApJ, 703, 1939
Williams, B. F. 2003, AJ, 126, 1312